Supplementary Information

Title:

Near-infrared imaging in fission yeast by genetically encoded biosynthesis of phycocyanobilin

Running Title:

iRFP imaging in fission yeast

Authors:

Keiichiro Sakai,[1,2,3] Yohei Kondo,[1,2,3] Hiroyoshi Fujioka,[4] Mako Kamiya,[5] Kazuhiro Aoki,[1,2,3,*] , and Yuhei Goto,[1,2,3,6*]

Affiliations:

[1]Quantitative Biology Research Group, Exploratory Research Center on Life and Living Systems (ExCELLS), National Institutes of Natural Sciences, 5-1 Higashiyama, Myodaiji-cho, Okazaki, Aichi 444-8787, Japan.

[2]Division of Quantitative Biology, National Institute for Basic Biology, National Institutes of Natural Sciences, 5-1 Higashiyama, Myodaiji-cho, Okazaki, Aichi 444-8787, Japan.

[3]Department of Basic Biology, School of Life Science, SOKENDAI (The Graduate University for Advanced Studies), 5-1 Higashiyama, Myodaiji-cho, Okazaki, Aichi 444-8787, Japan.

[4]Graduate School of Pharmaceutical Sciences, The University of Tokyo, 7-3-1 Hongo, Bunkyo-ku, Tokyo 113-0033, Japan.

[5]Graduate School of Medicine, The University of Tokyo, 7-3-1 Hongo, Bunkyo-ku, Tokyo 113-0033, Japan

[6]Lead contact

*Corresponding authors

*Correspondence: k-aoki@nibb.ac.jp and y-goto@nibb.ac.jp

Supplementary Figures

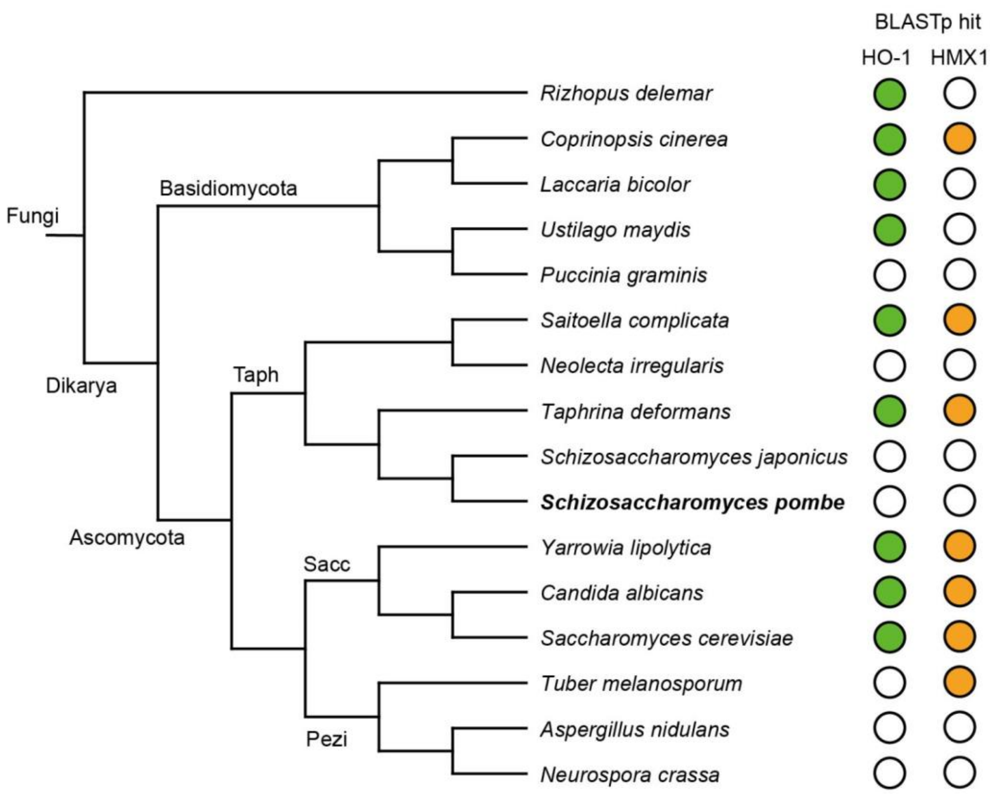

Fig. S1. Phylogenetic distribution of HO-like sequences in fungal species
Search results for heme oxygenase (HO)-like protein sequences in representative fungal species. Taph, Taphrinomycotina. Sacc, Saccharomycotina. Pezi, Pezizomycotina. The green circles indicate hits by BLASTp (e-value < 1e-5) with human HO1 as the query. The orange circles came from the same procedure except that *S.cerevisiae* HMX1 was the query.

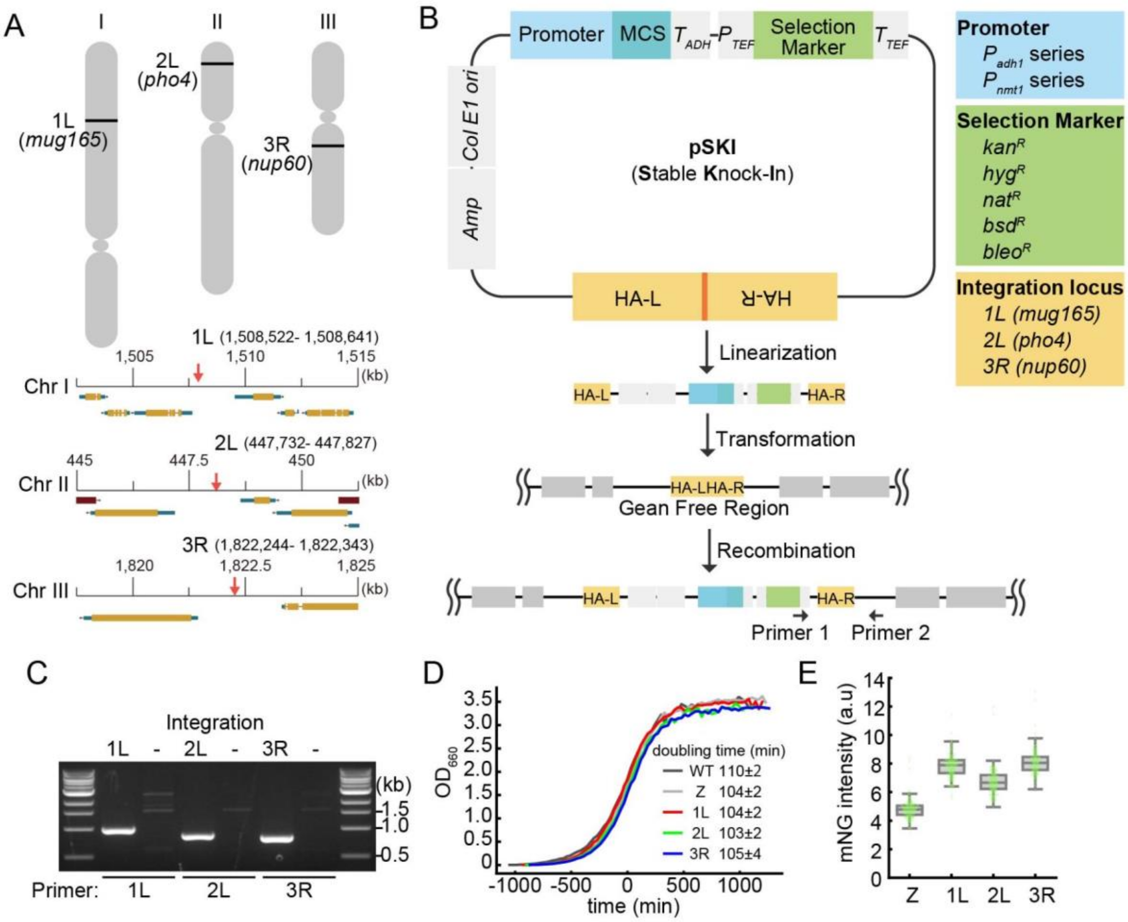

Fig. S2. Novel chromosome integration plasmids, pSKI, for *Schizosaccharomyces pombe*.
(A) Integration loci at the gene-free region of each chromosome (upper) and gene locations around integration loci (lower). Red arrows indicate the integration sites of each chromosome. (B) Plasmid map and integration procedure. The homology arm left and right (HA-L and HA-R) are connected with restriction enzyme recognition sites for linearization. Following linearization of the plasmid, DNA is introduced into the fission yeast cells by standard transformation procedures. Transformed DNA is integrated into the gene-free region through homologous recombination. The plasmid list is shown in Table S1. (C) Verification of the integration into each locus by PCR using primers 1 and 2 as indicated in panel B. Primer 1, which binds to the T_{TEF} region, is common to all three loci (1L, 2L, and 3R), while primer 2, which binds to the outside of HA-R, is specific to each locus. (D) Representative growth curve of strains integrated with empty vectors of each locus. Mean doubling times are shown with the S.D. (n = 3, independent experiments). The calculation of the doubling time is described in teh Materials and Methods. (E) Comparison of protein expression levels among 1L, 2L, 3R, and Z loci. mNeonGreen (mNG) was expressed from the indicated integration loci, and fluorescence intensity was quantified. Each dot represents the mNG fluorescence of a single cell with a boxplot, in which the box shows the quartiles of data with the whiskers denoting the minimum and maximum except for the outliers detected by 1.5 times the interquartile range (n > 150 cells).

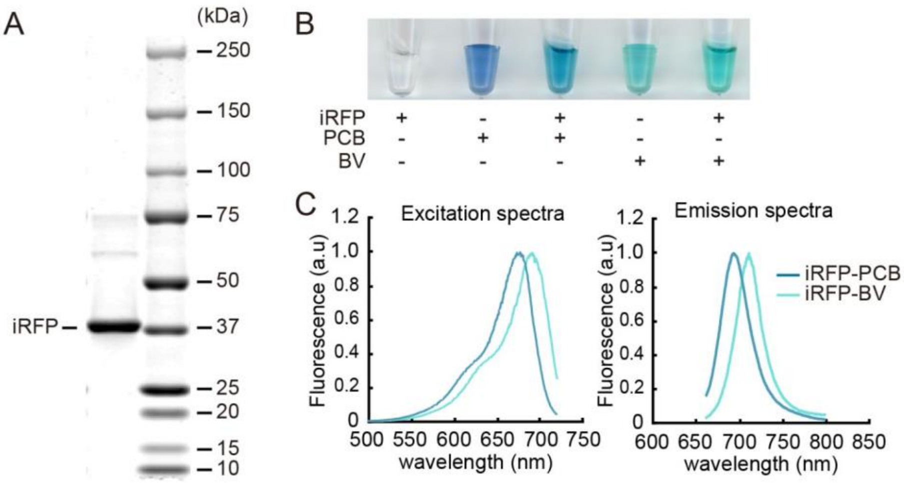

Fig. S3. PCB binds to iRFP *in vitro*

(A) A representative image of CBB staining of purified recombinant His-iRFP (39 kDa). (B) A photograph of the purified His-iRFP, free PCB, PCB-bound His-iRFP, free BV, and BV-bound His-iRFP. Of note, unbound BV or PCB was eluted during the process of the size exclusion chromatography. (C) Excitation (left) and emission (right) spectra of His-iRFP bound to BV or PCB. The fluorescence intensities are normalized by the peak intensities.

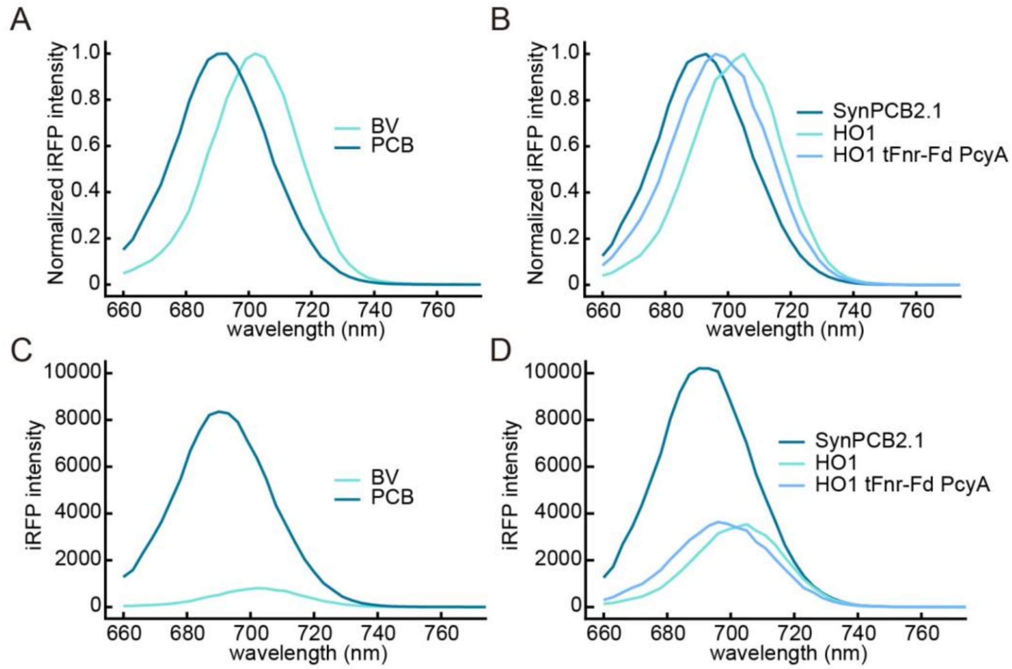

E

	Emission maximum (nm)
BV	702
PCB	690
SynPCB2.1	690
HO1	705
HO1 tFnr-Fd PcyA	696

Fig. S4. Emission spectra of iRFP-BV or iRFP-PCB *in vivo*

(A) Normalized emission spectra of iRFP-BV and iRFP-PCB in fission yeast cells expressing NLS-iRFP-NLS treated with BV (125 μM) and PCB (125 μM), respectively. Fission yeast cells were excited by a 640 nm laser light source, and emission was measured every 3 nm with a 20 nm window. The fluorescence intensity at each window was averaged from over 10 cells. The fluorescence intensities were divided by the peak intensity for the normalization. (B) Normalized emission spectra of fission yeast cells expressing SynPCB2.1, HO1, or three genes (HO1, tFnr-Fd, and PcyA). (C and D) Raw emission spectra of panel A (C) and panel B (D). (E) Summary table of emission peaks *in vivo*.

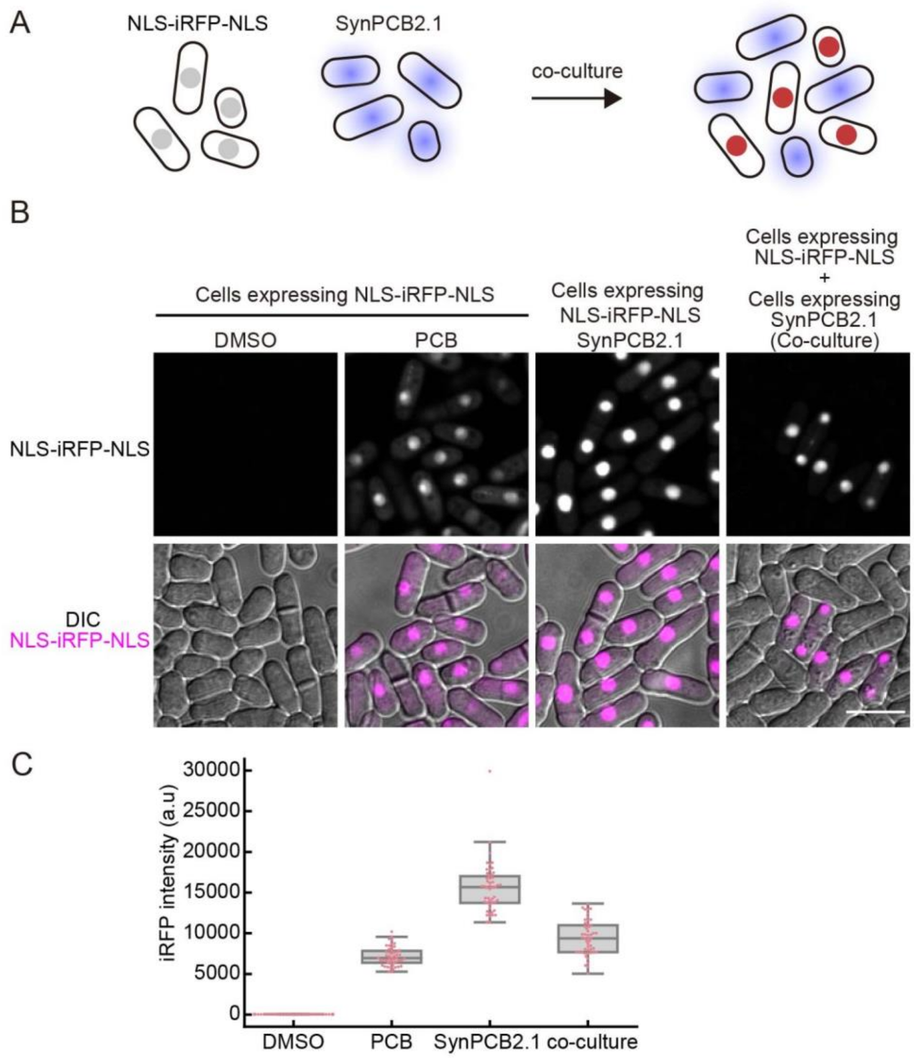

Fig. S5. PCB is leaked from fission yeast cells expressing SynPCB2.1.

(A) Schematic illustration of the co-culture experiment. Neither cells expressing only SynPCB2.1 nor cells expressing only NLS-iRFP-NLS exhibit iRFP fluorescence. NLS-iRFP-NLS exhibits iRFP fluorescence when the two cell lines are co-cultured due to the leaking of PCB from cells into the culture media. (B) Representative images of cells expressing NLS-iRFP-NLS treated with DMSO (first column), PCB (125 μM, second column), co-expression of SynPCB2.1 (third column), and co-culture with cells expressing SynPCB2.1 (fourth column). Scale bar, 10 μm. (C) Quantification of NLS-iRFP-NLS signal intensity in panel B. Single-cell fluorescence intensities are shown by dots with boxplots, in which the box shows the quartiles of data with the whiskers denoting the minimum and maximum except for the outliers detected by 1.5 times the interquartile range (n = 50 cells).

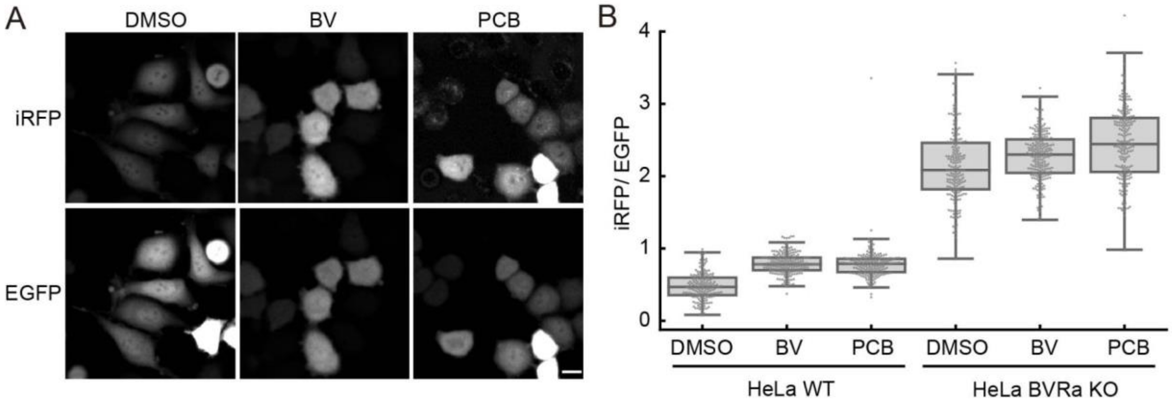

Fig. S6. iRFP fluorescence in mammalian cells treated with PCB or BV
(A) Representative images of parental HeLa cells expressing iRFP-P2A-EGFP treated with DMSO, BV (25 μM), or PCB (25 μM). Scale bar, 10 μm. (B) Quantification of iRFP/EGFP values in HeLa cells and HeLa/BVRA KO cells under the indicated conditions. Each dot represents a data point from a single cell with a boxplot, in which the box shows the quartiles of data with the whiskers denoting the minimum and maximum except for the outliers detected by 1.5 times the interquartile range (n > 170 cells).

Table S1. Plasmid list

Plasmid name	Description	Source	Benchling Link
pSKI-KAN-1L-A1-M	pSKI	this study	https://benchling.com/s/seq-G3P9JqxX51ObX5Sz96MA
pSKI-NAT-1L-A1-M	pSKI	this study	https://benchling.com/s/seq-8eBCjMRKikhCkkluJGhWW
pSKI-BSD-1L-A1-M	pSKI	this study	https://benchling.com/s/seq-HhBJcOmn70PBjUtaRdFR
pSKI-BLE-1L-A1-M	pSKI	this study	https://benchling.com/s/seq-bhdt76l7rpG8s7St32bv
pSKI-KAN-2L-A1-M	pSKI	this study	https://benchling.com/s/seq-TreXp3COB6wHS3lOhASP
pSKI-NAT-2L-A1-M	pSKI	this study	https://benchling.com/s/seq-HLDrXgZxwWWQzFpCQmxk
pSKI-BSD-2L-A1-M	pSKI	this study	https://benchling.com/s/seq-eDFPR3eDDbwOpHn3wELo
pSKI-BLE-2L-A1-M	pSKI	this study	https://benchling.com/s/seq-tU4cqJD4RsS3y9AFcgvD
pSKI-KAN-3R-A1-M	pSKI	this study	https://benchling.com/s/seq-QLwzrxGXyx0TpSjNMzAH
pSKI-NAT-3R-A1-M	pSKI	this study	https://benchling.com/s/seq-Hvoe4y6Rfz9HRKKXmM8Q
pSKI-HYG-3R-A1-M	pSKI	this study	https://benchling.com/s/seq-EkO6jh5uMmuXF5brQFBq
pSKI-BSD-3R-A1-M	pSKI	this study	https://benchling.com/s/seq-NUrSW450XbywsQzxnyX9
pSKI-BLE-3R-A1-M	pSKI	this study	https://benchling.com/s/seq-G4LydqOGtHxT2v7SHikY
pSKI-KAN-1L-N1	pSKI	this study	https://benchling.com/s/seq-lajqCWRwNsuhe2ckb9nk
pSKI-NAT-1L-N1	pSKI	this study	https://benchling.com/s/seq-X1w13cdTQVw4wgGpBfZR
pSKI-BSD-1L-N1	pSKI	this study	https://benchling.com/s/seq-QQZRlvatv7zHfuA7bMnI
pSKI-BLE-1L-N1	pSKI	this study	https://benchling.com/s/seq-MfQgtyoBCoIVSDIujzjg
pSKI-KAN-2L-N1	pSKI	this study	https://benchling.com/s/seq-CFloX6NrLvuJrnI5JaPD
pSKI-NAT-2L-N1	pSKI	this study	https://benchling.com/s/seq-YbDO5EX4oqDfJJguRrf0
pSKI-HYG-2L-N1	pSKI	this study	https://benchling.com/s/seq-8e48M8moxUXOqsybHbYO
pSKI-BSD-2L-N1	pSKI	this study	https://benchling.com/s/seq-a5dfK1ki5ow43Px6o0tl
pSKI-BLE-2L-N1	pSKI	this study	https://benchling.com/s/seq-KocnJoOdrJwaDPHHGeke

pSKI-KAN-3R-N1	pSKI	this study	https://benchling.com/s/seq-BZmnME31WCynpEwW7GfH
pSKI-NAT-3R-N1	pSKI	this study	https://benchling.com/s/seq-kVuyYx3nHglfwjYI0MYPP
pSKI-BSD-3R-N1	pSKI	this study	https://benchling.com/s/seq-7M97ws9s2eY5ZfqXlQBq
pSKI-HYG-3R-N1	pSKI	this study	https://benchling.com/s/seq-1eL7D3ki8KLvb3Uh3etM
pSKI-BLE-3R-N1	pSKI	this study	https://benchling.com/s/seq-kMwFYBeWLuaYDoegFvdl
pFA6a-iRFP-kan	iRFP C-terminal tagging	this study	https://benchling.com/s/seq-bkYIYdFO0LlSWLRgqKf2
pFA6a-iRFP-hyg	iRFP C-terminal tagging	this study	https://benchling.com/s/seq-emc65aNbjBFYkdt8Ooib
pFA6a-iRFP-nat	iRFP C-terminal tagging	this study	https://benchling.com/s/seq-hb5KLMGZXpgTFmQN9MH5
pFA6a-iRFP-bsd	iRFP C-terminal tagging	this study	https://benchling.com/s/seq-MB0yvsIASTKHVyJnvflU
pFA6a-mNeonGreen (S.p codon optimized)-kan	mNG C-terminal tagging	this study	https://benchling.com/s/seq-r5vPvd2m4SeMm6VxVhiN
pSKI-KAN-1L-A1-M-SynPCB2.1	synPCB2.1	this study	https://benchling.com/s/seq-iAht1qGQ6taledZRBjhy
pSKI-NAT-1L-A1-M-SynPCB2.2	synPCB2.1	this study	https://benchling.com/s/seq-6Ds1klA3foLeFGMjNRY4
pSKI-BSD-1L-A1-M-SynPCB2.1	synPCB2.1	this study	https://benchling.com/s/seq-t5O2P2WzKmrmTYCcEtUk
pSKI-BLE-1L-A1-M-SynPCB2.1	synPCB2.1	this study	https://benchling.com/s/seq-TeeZbKcTCjCZxRoCQ9ua
pSKI-BSD-1L-A1-M-SynPCB2.1-Lifeact-iRFP	pSKI-SynPCB2.1-Lifeact-iRFP	this study	https://benchling.com/s/seq-kazB0PhzppnUokAcnZBp
pSKI-BSD-1L-A1-M-SynPCB2.1-Tadh1-Padh1-NLS-iRFP-NLS-Tadh1	pSKI-SynPCB2.1-NLS-iRFP-NLS	this study	https://benchling.com/s/seq-gGVpZDolap5t4mj7bGFK
pSKI-BSD-2L-A1-M-NLS-iRFP-NLS		this study	https://benchling.com/s/seq-obPOLIX96PllBreCKNXY
pSKI-NAT-1L-A1-M-MTS-HO1		this study	https://benchling.com/s/seq-A38a1P9LQU1mhRfdWPBb
pSKI-NAT-3R-A1-M-MTS-btFnr-bFd		this study	https://benchling.com/s/seq-6MjlWH76M7373w9WG02R
pMNATZA1-MTS-PcyA		this study	https://benchling.com/s/seq-sRCmN6qpFCs6Dp5yVqzO
pSKI-KAN-1L-A1-M-MTS-HO1		this study	https://benchling.com/s/seq-U8xwbETwRXjlZmqHhQ2O
pSKI-KAN-3R-A1-M-MTS-btFnr-bFd		this study	https://benchling.com/s/seq-SuqW1exP3iAJHvnDvxeD
pMNATZA1		this study	https://benchling.com/s/seq-F7zeXNTMu66Gs0zKvIpx

pMNATZA1-spmNeonGreen		this study	https://benchling.com/s/seq-eNXfcf6oImjRKuJpX9k5
pSKI-NAT-1L-A1-M-spmNeonGreen (S.p codon optimized)		this study	https://benchling.com/s/seq-5RTHLQjGhwtHW5hpF9XC
pSKI-NAT-2L-A1-M-spmNeonGreen (S.p codon optimized)		this study	https://benchling.com/s/seq-5KTJy6ykRRzXgNaRUUeV
pSKI-NAT-3R-A1-M-spmNeonGreen (S.p codon optimized)		this study	https://benchling.com/s/seq-8eBCjMRKikhCkkluJGhW
pNATZA15-mCherry-atb2		this study	https://benchling.com/s/seq-0XMOLayGLNMT0Jx5xFa8
pHBCA11-NLS-mTagBFP2-NLS		this study	https://benchling.com/s/seq-vsO72fejJfzTcSFPqF5X
pMBLE-3R-A1-Turquoise2-GL-ras1delN200		This study	https://benchling.com/s/seq-KXyKpjnMwc3D1kstue68
pCold-TEV-iRFP713		this study	https://benchling.com/s/seq-2HCLXjM6wnXr2mMIa5QH
pCAGGS-iRFP-P2A-EGFP		this study	https://benchling.com/s/seq-CwGlEm2qwVg6M8Cq2fVL

Table S2. ***Schizosaccharomyces pombe*** **strain list**

Strain name	Genotype	Fig.	Source
L972	h-	Fig. 2C, 2D, Fig. S2C, S2D	NBRP
L975	h+		NBRP
SK276	h- 2L::Padh1-NLS-iRFP-NLS<<bsd	Fig. 1B, 1C, 1D, Fig. 2B, 2C, 2D, Fig. 3B, 3C, 3G, Fig. S4A, S4C, Fig. S5B, S5C	this study, L972
SK277	h+ 2L::Padh1-NLS-iRFP-NLS<<bsd		this study, L975
SK284	h- 2L::Padh1-NLS-iRFP-NLS<<bsd 1L::Padh1-HO1<<nat	Fig. 2B, Fig. 3B, 3C, 3G, Fig. S4B, S4D	this study, SK276
SK285	h+ 2L::Padh1-NLS-iRFP-NLS<<bsd 3R::Padh1-btFnr-bFd<<nat	Fig. 2B	this study, SK277
SK287	h+ 2L::Padh1-NLS-iRFP-NLS<<bsd z::Padh1-PcyA<<nat	Fig. 2B	this study, SK277
SK294	h- 2L::Padh1-NLS-iRFP-NLS<<bsd 1L::Padh1-HO1<<nat 3R::Padh1-btFnr-bFd<<kan	Fig. 2B	this study, SK284
SK296	h+ 2L::Padh1-NLS-iRFP-NLS<<bsd z::Padh1-PcyA<<nat 1L::Padh1-HO1<<kan	Fig. 2B	this study, SK287
SK295	h+ 2L::Padh1-NLS-iRFP-NLS<<bsd z::Padh1-PcyA<<nat 3R::Padh1-btFnr-bFd<<kan	Fig. 2B	this study, SK287
SK305	h+ 2L::Padh1-NLS-iRFP-NLS<<bsd 1L::Padh1-HO1<<nat 3R::Padh1-btFnr-bFd<<kan z::Padh1-PcyA<<nat	Fig. 2B, Fig. 3G, Fig. S4B, S4D	this study, SK294 x SK295
SK282	h- 2L::Padh1-NLS-iRFP-NLS<<bsd 1L::Padh1-SynPCB2.1<<kan	Fig. 3G, Fig. S4B, S4D, Fig. S5B, S5C	this study, SK276
YG658	h- 1L::Padh1-SynPCB2.1<<bsd		this study, L972
YG1074	h- 1L::Padh1-SynPCB2.1<<bsd cdc2-iRFP<<kan	Fig. 4B	this study, YG658
YG1096	h- 1L::Padh1-SynPCB2.1<<bsd rpb9-iRFP<<kan	Fig. 4B	this study, YG658
YG1095	h- 1L::Padh1-SynPCB2.1<<bsd rpa49-iRFP<<kan	Fig. 4B	this study, YG658
YG1085	h- 1L::Padh1-SynPCB2.1<<bsd swi6-iRFP<<kan	Fig. 4B	this study, YG658
YG1093	h- 1L::Padh1-SynPCB2.1<<bsd pds5-iRFP<<kan	Fig. 4B	this study, YG658
YG1083	h- 1L::Padh1-SynPCB2.1<<bsd cut11-iRFP<<kan	Fig. 4B	this study, YG658
YG1094	h- 1L::Padh1-SynPCB2.1<<bsd mal3-iRFP<<kan	Fig. 4B	this study, YG658
YG1084	h- 1L::Padh1-SynPCB2.1<<bsd sfi1-iRFP<<kan	Fig. 4B	this study, YG658

YG1086	h- 1L::Padh1-SynPCB2.1<<bsd cox4-iRFP<<kan	Fig. 4B	this study, YG658
YG1092	h- 1L::Padh1-SynPCB2.1<<bsd cnx1-iRFP<<kan	Fig. 4B	this study, YG658
SK323	h- 1L::Padh1-SynPCB2.1-Lifeact-iRFP<<bsd	Fig. 5A	this study, L972
YG1082	h- 1L::Padh1-synPCB2.1-Tadh1-Padh1-NLS-iRFP-NLS-Tadh1<<bsd	Fig. 5B	this study, L972
SK356	h- 3R::Padh1-spnTurquoise2-GL-ras1delN200<<ble		this study, L972
YG1114	h- 3R::Padh1-spnTurquoise2-GL-ras1delN200<<ble mis12-spmNeonGreen<<kan 1L::Padh1-synPCB2.1-Lifeact-iRFP<<bsd		this study, SK356
YG1124	h- 3R::Padh1-spnTurquoise2-GL-ras1delN200<<ble mis12-spmNeonGreen<<kan 1L::Padh1-synPCB2.1-Lifeact-iRFP<<bsd z::Padh15-mCherry-atb2<<nat		this study, YG1114
YG1127	h- 3R::Padh1-Turquoise2-GL-ras1delN200<<ble mis12-spmNeonGreen<<kan 1L::Padh1-synPCB2.1-Lifeact-iRFP<<bsd z::Padh15-mCherry-atb2<<nat c::Padh11-NLS-mTagBFP2-NLS<<hyg	Fig. 5C	this study, YG1124
SK064	h- 1L::Padh1<<nat	Fig. S2C, S2D	this study, L972
SK098	h- 2L::Padh1<<nat	Fig. S2C, S2D	this study, L972
SK100	h- 3R::Padh1<<nat	Fig. S2C, S2D	this study, L972
SK062	h- z::Padh1<<nat	Fig. S2D	this study, L972
SK063	h- z::Padh1-spmNeonGreen<<nat	Fig. S2E	this study, L972
SK027	h- 1L::Padh1-spmNeonGreen<<nat	Fig. S2E	this study, L972
SK099	h- 2L::Padh1-spmNeonGreen<<nat	Fig. S2E	this study, L972
SK101	h- 3R::Padh1-spmNeonGreen<<nat	Fig. S2E	this study, L972
YG503	h- 1L::Padh1-SynPCB2.1<<kan	Fig. S5B, S5C	this study, L972

Table S3. Primer list

Primer name	Primer sequence (5' → 3')
TtefF	ATGCGAAGTTAAGTGCGCAG
1Llocus-check-R	TCGGATAGTAGTTGCCAACAGC
2Llocus-check-R	CGTATTTCGCTGTACATAGCATAATTTC
3Rlocus-check-R	TGCAGCTGTAGTAAATTTCGAAGTC

Table S4. Genome information and BLASTp results

Species	BLASTp e-value (HO-1)	BLASTp e-value (HMX1)	Accession No.	Reference
Rhizopus delemar RA 99-880	5.19E-53		GCA_000149305.1	(Ma et al., 2009)
Coprinopsis cinerea Okayama-7	1.89E-31	2.89E-07	GCA_000182895.1	(Stajich et al., 2010)
Laccaria bicolor S238N-H82	1.51E-30		GCA_000143565.1	(Martin et al., 2008)
Ustilago maydis strain 521	5.92E-15		GCA_000328475.2	(Kämper et al., 2006)
Puccinia graminis f. sp. tritici strain CRL 75-36-700-3			GCA_000149925.1	(Duplessis et al., 2011)
Saitoella complicata NRRL Y-17804	5.58E-13	1.03E-27	GCA_001661265.1	(Riley et al., 2016)
Neolecta irregularis DAH-3			GCA_001929475.1	(Nguyen et al., 2017)
Taphrina deformans PYCC 5710	4.16E-08	9.95E-24	GCA_000312925.2	(Cissé et al., 2013)
Schizosaccharomyces japonicus yFS275			GCA_000149845.2	(Rhind et al., 2011)
Schizosaccharomyces pombe L972			GCA_000002945.2	(Wood et al., 2002)
Yarrowia lipolytica	6.73E-10	7.60E-63	GCA_000002525.1	(Dujon et al., 2004)
Candida albicans WO-1	9.74E-12	8.36E-56	GCA_000149445.2	(Butler et al., 2009)
Saccharomyces cerevisiae S288C	6.52E-09	0	GCA_000146045.2	(Goffeau et al., 1996)
Tuber melanosporum Mel28		1.07E-22	GCA_000151645.1	(Martin et al., 2010)
Aspergillus nidulans FGSC-A4			GCA_000149205.2	(Arnaud et al., 2012)
Neurospora crassa OR74A			GCA_000182925.2	(Galagan et al., 2003)

Supplementary Reference

Arnaud, M. B., Cerqueira, G. C., Inglis, D. O., Skrzypek, M. S., Binkley, J., Chibucos, M. C., Crabtree, J., Howarth, C., Orvis, J., Shah, P., et al. (2012). The Aspergillus Genome Database (AspGD): recent developments in comprehensive multispecies curation, comparative genomics and community resources. *Nucleic Acids Res.* **40**, D653–9.

Butler, G., Rasmussen, M. D., Lin, M. F., Santos, M. A. S., Sakthikumar, S., Munro, C. A., Rheinbay, E., Grabherr, M., Forche, A., Reedy, J. L., et al. (2009). Evolution of pathogenicity and sexual reproduction in eight Candida genomes. *Nature* **459**, 657–662.

Cissé, O. H., Almeida, J. M. G. C. F., Fonseca, A., Kumar, A. A., Salojärvi, J., Overmyer, K., Hauser, P. M. and Pagni, M. (2013). Genome sequencing of the plant pathogen Taphrina deformans, the causal agent of peach leaf curl. *MBio* **4**, e00055–13.

Dujon, B., Sherman, D., Fischer, G., Durrens, P., Casaregola, S., Lafontaine, I., De Montigny, J., Marck, C., Neuvéglise, C., Talla, E., et al. (2004). Genome evolution in yeasts. *Nature* **430**, 35–44.

Duplessis, S., Cuomo, C. A., Lin, Y.-C., Aerts, A., Tisserant, E., Veneault-Fourrey, C., Joly, D. L., Hacquard, S., Amselem, J., Cantarel, B. L., et al. (2011). Obligate biotrophy features unraveled by the genomic analysis of rust fungi. *Proc. Natl. Acad. Sci. U. S. A.* **108**, 9166–9171.

Galagan, J. E., Calvo, S. E., Borkovich, K. A., Selker, E. U., Read, N. D., Jaffe, D., FitzHugh, W., Ma, L.-J., Smirnov, S., Purcell, S., et al. (2003). The genome sequence of the filamentous fungus Neurospora crassa. *Nature* **422**, 859–868.

Goffeau, A., Barrell, B. G., Bussey, H., Davis, R. W., Dujon, B., Feldmann, H., Galibert, F., Hoheisel, J. D., Jacq, C., Johnston, M., et al. (1996). Life with 6000 genes. *Science* **274**, 546, 563–7.

Kämper, J., Kahmann, R., Bölker, M., Ma, L.-J., Brefort, T., Saville, B. J., Banuett, F., Kronstad, J. W., Gold, S. E., Müller, O., et al. (2006). Insights from the genome of the biotrophic fungal plant pathogen Ustilago maydis. *Nature* **444**, 97–101.

Ma, L.-J., Ibrahim, A. S., Skory, C., Grabherr, M. G., Burger, G., Butler, M., Elias, M., Idnurm, A., Lang, B. F., Sone, T., et al. (2009). Genomic analysis of the basal lineage fungus Rhizopus oryzae reveals a whole-genome duplication. *PLoS Genet.* **5**, e1000549.

Martin, F., Aerts, A., Ahrén, D., Brun, A., Danchin, E. G. J., Duchaussoy, F., Gibon, J., Kohler, A., Lindquist, E., Pereda, V., et al. (2008). The genome of Laccaria bicolor provides insights into mycorrhizal symbiosis. *Nature* **452**, 88–92.

Martin, F., Kohler, A., Murat, C., Balestrini, R., Coutinho, P. M., Jaillon, O., Montanini, B., Morin, E., Noel, B., Percudani, R., et al. (2010). Périgord black truffle genome uncovers evolutionary origins and mechanisms of symbiosis. *Nature* **464**, 1033–1038.

Nguyen, T. A., Cissé, O. H., Yun Wong, J., Zheng, P., Hewitt, D., Nowrousian, M., Stajich, J. E. and Jedd, G. (2017). Innovation and constraint leading to complex multicellularity in the Ascomycota. *Nat. Commun.* **8**, 14444.

Rhind, N., Chen, Z., Yassour, M., Thompson, D. A., Haas, B. J., Habib, N., Wapinski, I., Roy, S., Lin, M. F., Heiman, D. I., et al. (2011). Comparative functional genomics of the fission yeasts. *Science* **332**, 930–936.

Riley, R., Haridas, S., Wolfe, K. H., Lopes, M. R., Hittinger, C. T., Göker, M., Salamov, A. A., Wisecaver, J. H., Long, T. M., Calvey, C. H., et al. (2016). Comparative genomics of biotechnologically important yeasts. *Proc. Natl. Acad. Sci. U. S. A.* **113**, 9882–9887.

Stajich, J. E., Wilke, S. K., Ahrén, D., Au, C. H., Birren, B. W., Borodovsky, M., Burns, C., Canbäck, B., Casselton, L. A., Cheng, C. K., et al. (2010). Insights into evolution of multicellular fungi from the assembled chromosomes of the mushroom Coprinopsis cinerea (Coprinus cinereus). *Proc. Natl. Acad. Sci. U. S. A.* **107**, 11889–11894.

Vještica, A., Marek, M., Nkosi, P. J., Merlini, L., Liu, G., Bérard, M., Billault-Chaumartin, I. and Martin, S. G. (2020). A toolbox of stable integration vectors in the fission yeast Schizosaccharomyces pombe. *J. Cell Sci.* **133**,.

Wood, V., Gwilliam, R., Rajandream, M.-A., Lyne, M., Lyne, R., Stewart, A., Sgouros, J., Peat, N., Hayles, J., Baker, S., et al. (2002). The genome sequence of Schizosaccharomyces pombe. *Nature* **415**, 871–880.